JOURNAL OF THERMOPHYSICS AND HEAT TRANSFER
Vol. 12, No. 2, April–June 1998

Thermal Energy Accommodation from Oxygen Atoms Recombination on Metallic Surfaces

P. Cauquot,* S. Cavadias,† and J. Amouroux‡
Université Pierre et Marie Curie, Paris 75005, France

Measurements of recombination and accommodation coefficients of oxygen atoms are important in determining the energy released to spacecraft thermal protection during the atmospheric entry phase. The aim of this work is the evaluation of the accommodation of the energy released from oxygen atoms recombination on metals such as copper, silver, cobalt, zinc, nickel, gold, and steel with a calorimetric method and its evolution with the surface temperature. The chemical evolution of the surface of the material (oxidation) is followed by electron spectroscopy for chemical analysis for different exposure times to the oxygen atoms flux. A catalycity scale of the materials was established and their catalycity was correlated with their electronic properties (*n*- or *p*-type semiconductivity).

Nomenclature

D = dissociation energy of the molecule, J mol^{-1}
D_O = oxygen dissociation energy, 4.85×10^5 J mol^{-1}
E_a = adsorption energy of an atom, J mol^{-1}
E_{ER} = activation energy of the Eley–Rideal mechanism, J mol^{-1}
E_{LH} = activation energy of the Langmuir–Hinshelwood mechanism, J mol^{-1}
E_m = dissociative adsorption energy of a molecule, J mol^{-1}
k = Boltzmann constant, J K^{-1}
m = mass of an oxygen atom, kg
N_A = Avogadro number, atoms mol^{-1}
n_0 = total adsorption site density, atoms cm^{-3}
T = surface temperature, K
v = frequency factor of the Langmuir–Hinshelwood process, s^{-1}
Z_a = atoms flux, atoms cm^{-3} s^{-1}
Z_m = molecules flux, mol cm^{-3} s^{-1}
Δn = number of oxygen atoms consumed per time unit, atoms s^{-1}
δQ = energy released to the surface by recombination per time unit, J s^{-1}
γ^* = recombination coefficient for the Eley–Rideal mechanism
θ = coverage of adsorbed atoms

I. Introduction

THE energy released during atom recombination on a surface is shared between the produced molecules and the surface. The transfer of this energy to the surface leads to its heating. The number of recombined atoms and the energy transferred depends on the nature of the surface, and the process is referred to be a catalytic atom recombination. When the recombination species are oxygen atoms, the very high sticking coefficient leads to the formation of an oxide layer on the surface. In a few milliseconds, a modification of the nature of the surface and its properties occurs. The quick aging of the material results in a change of its catalycity. These studies are very important for the conception of catalytic materials and the qualification of materials supporting high thermal constraints.[1]

Reliable experimental procedures are needed to develop models and simulations to study the typical flow on the airfoil and quantify the heat transfer in the frozen layer around the material.[2–4] There are very few available experimental data on the recombination coefficient γ and accommodation coefficient β of oxygen or nitrogen atoms on different kinds of industrial refractory materials. Results are needed to express k_w (called catalycity) of the material that measures the whole heat transfer to the surface.

The experimental data on atomic oxygen recombination coefficients γ have been established on ceramic and metallic materials without taking into account the aging of the material (oxidation and ablation) or with an unknown degree of purity (surface metallic impurities, organic pollutions).[5–11] The experimental data of β are few and have been established only on metallic surfaces[6,12] without performing any surface analyses.

Also, the operating procedures need to be compared to establish reliable values. Melin and Madix[6] measured accommodation coefficients on metallic surfaces with a maximum accuracy of 30%, whereas Krech[12] obtained β values for high-velocity atomic oxygen (8 km s^{-1}) by infrared measurements of the heated surfaces. None of these methods take into account the purity of the material and the variation of surface composition during the measurement.

Our approach in this paper is the evaluation of the accommodation of the energy released from oxygen atoms recombination on metals such as copper, silver, cobalt, zinc, nickel, gold, and steel. The objective of this work is improvement in the accuracy of the results and the establishment of a catalycity scale. Moreover, metallic thermal protection systems are being considered for next-generation reusable launch vehicles.[13] The surfaces are assumed to be nonevolutive during the experiment, this means that no surface reaction occurs except for the recombination reaction.

The operating procedure consists of the production of an atomic oxygen flow in a low-pressure microwave plasma reactor. The heat flux resulting from the atomic recombination on the test target is measured by calorimetry. Knowing the atomic oxygen flux that recombines on the surface, the accommodation coefficient is determined for each material at a constant temperature. One of the advantages of the method is that the radiation losses are the same during the measurements be-

Received July 17, 1997; revision received Oct. 24, 1997; accepted for publication Oct. 24, 1997.

*Research Scientist, Laboratoire de Génie des Procédés Plasma, Ecole Nationale Supérieure de Chimie de Paris.

†Associate Professor, Laboratoire de Génie des Procédés Plasma, Ecole Nationale Supérieure de Chimie de Paris.

‡Professor, Laboratoire de Génie des Procédés Plasma, Ecole Nationale Supérieure de Chimie de Paris, 11, rue Pierre et Marie Curie, 75231 Paris Cedex 05, France.

cause the surface temperature is always constant. The modification of the chemical composition of the surface of the material is followed by electron spectroscopy for chemical analysis (ESCA) for different exposure times to the oxygen plasma.

In this paper, the theoretical principle of the oxygen atoms recombination and the energy transfer will be first summarized in Sec. II. The experimental setup will be detailed in Sec. III and both catalycity results and characterization of the material's surface will be presented in Sec. IV. Finally, correlations between the electronic properties of the materials and their catalycity will be the aim of the discussion in Sec. V.

II. Theoretical Background

A. Mass Transfer to the Surface

When oxygen atoms hit a surface, different kinds of reactions occur on the surface of the material. These atoms can be adsorbed on the surface and some oxidation mechanisms, ablation of the material, diffusion of oxygen into the bulk material, and catalytic recombination of oxygen atoms can occur. These different processes leading to the oxygen atoms losses are schematized in Figs. 1 and 2.

It is well known that the adsorption of molecular oxygen on a metal leads to its oxidation. As the chemical potential of the atomic oxygen is greater than those of molecular oxygen, atomic oxygen will form oxygen species strongly linked to the metal. The interaction between oxygen atoms and a metallic surface could also form an oxide layer that will have different chemical properties than the nonoxided metal.

The formation of bonds between the metallic element and oxygen can be responsible for the ablation of the material. Indeed, if the metallic oxide that is formed is volatile, it could be extracted from the bulk metal and be evaporated in the gas. This process is all the more probable when the surface temperature of the material is high.

If the solubility of oxygen into the metal is high, the oxygen atoms could diffuse into the bulk material. The diffusion coefficient of oxygen into a metal can be expressed by the following Arrhenius function:

$$D = D_O e^{-E_D/RT}$$

where E_D is the activation energy of the process. Thus, diffusion into the bulk metal becomes a nonneglected process when the surface temperature of the material is high.

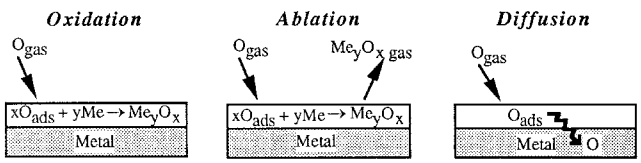

Fig. 1 Reaction mechanisms during the interaction of oxygen atoms with metals.

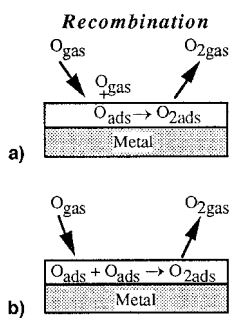

Fig. 2 O-atoms recombination on metallic surfaces: a) ER and b) LH mechanisms.

When oxygen atoms strike a surface some recombination reactions occur. The reaction mechanisms can be considered as three steps: 1) the atomic adsorption step, 2) the recombination step, and 3) the molecular desorption step. The recombination and desorption steps are indissociably linked because the formation energy of the O_2 molecule bound is partially used during the desorption phase. The atoms are adsorbed on the active sites of the material surface that acts like a catalyst. There are two possible reaction paths for the recombination of atoms on a surface. Considering the first reaction path, a gas atom near the surface reacts with an adsorbed atom to form a molecule that desorbs immediately, releasing one active site. This is called the Eley–Rideal (ER) mechanism (Fig. 2a). The second reaction path describes the reaction between two adsorbed atoms to form a molecule that desorbs into the gas, releasing two active sites. This is called the Langmuir–Hinshelwood (LH) mechanism (Fig. 2b). Whichever mechanism occurs, the exothermic recombination reaction releases some energy that is transferred to the desorbed molecule and the surface. The chemical energy transfer during the atomic recombination process will depend on the recombination mechanism and on the nature of the reactive surface.

B. Recombination Energy Transfer

Figure 3 represents a potential energy diagram for the atomic and dissociative adsorption of a molecule, considering a process without any precursor state and without activation, according to Halpern and Rosner,[14] who studied the chemical energy accommodation mechanisms for *N*/transition metals systems. Assuming that atomic and dissociative chemisorption rates are respectively proportional to $(1 - \theta)$ and $(1 - \theta)^2$ with unit surface sticking probabilities, then, in the absence of appreciable atom desorption, the steady-state equation for θ can be written

$$Z_m(1 - \theta)^2 + Z_a(1 - \theta) = \gamma^* Z_a\theta + \nu n_0\theta^2 e^{-(E_{LH}/kT)} \quad (1)$$

Dividing Eq. (1) by the incident Z_a gives

$$\mu(1 - \theta)^2 + (1 - \theta) = \gamma^*\theta + \sigma\theta^2 \quad (2)$$

where μ and σ are defined by

$$\mu = Z_m/Z_a \quad \text{and} \quad \sigma = (\nu n_0/Z_a)e^{-(E_{LH}/kT)}$$

The overall surface atom γ can be found by summing the terms that describe the atom recombining by the ER and LH mechanisms and dividing by the incident Z_a

$$\gamma = \frac{Z_a(1 - \theta) + \gamma^* Z_a\theta}{Z_a} = 1 - \theta(1 - \gamma^*) \quad (3)$$

The atomic adsorption and molecular dissociative adsorption on a surface release E_m and E_a, respectively (Fig. 3). Moreover, a molecule formed by the recombination of atoms desorbs by

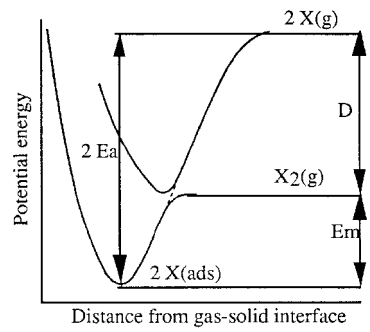

Fig. 3 Potential energy diagram for atomic and dissociative adsorption.

crossing an activation energy gate E_{ER} for an ER mechanism and E_{LH} for an LH mechanism. The accommodation coefficient of chemical energy β is the ratio of the energy transferred to the surface by the adsorption/recombination-desorption process and the total energy released by these reactions

$$\beta = \frac{\frac{1}{2}E_m\mu(1-\theta)^2 + E_a(1-\theta) - E_{ER}\theta\gamma^* - \frac{1}{2}E_{LH}\sigma\theta^2}{[1-\theta(1-\gamma^*)](D/2)} \quad (4)$$

In the numerator of Eq. (4), the first term is half of the heat of molecular dissociative adsorption and the second term is half of the heat of atomic adsorption. The last terms represent the energy removed by the molecule leaving the surface according to ER and LH mechanisms. The denominator is the overall heat released by the two processes.

Assuming δQ and Δn, Eq. (4) becomes

$$\beta = \frac{\delta Q}{\Delta n[(D/2)(1/N_A)]} \quad (5)$$

The principle of the accommodation coefficient measurement for an atomic oxygen flux consists of performing a heat and mass balance to determine the recombination energy transferred to the surface and the oxygen atoms flux that recombine on the surface. This method assumes that the recombination reaction is the only reaction process occurring between the incident oxygen atoms flux and the surface. Thus, the chemical state of the surface should not change during the experiment. This hypothesis of nonevolutive surfaces should be verified by controlling the chemical state of the materials for different exposure times to the oxygen plasma. Some appropriate surface chemical analyses could also validate the method and its limits.

The measurements under an atomic oxygen flux are based on a calorimetric method where the studied materials are used as isothermal calorimeters. It is carried out by a two-step process: in the first step, the sample, kept at a constant temperature by proportional, integral, and differential (PID) regulation, is exposed to an oxygen plasma free of oxygen atoms. At the same time, the electric power needed to keep the sample at this temperature is measured by an appropriate electronic device. In the second step, the same sample is exposed to an oxygen plasma including oxygen atoms. In this case, a part of the oxygen atoms is recombined on the sample surface and a part of the energy released from the recombination reaction is transferred to the surface. As the temperature is the same as in the first step and is regulated, the power supplied by the controller is less. The difference of power in the two cases is a result of the recombination of the oxygen atoms and represents the total energy transferred by recombination on all surfaces. An advantage of this method is that the radiation losses are the same in the two cases because the temperature remains constant. To calculate the elementary accommodation energy, we have to measure the number of atoms that recombine on the surface by performing a mass balance inlet/outlet in the reactor.

III. Experimental Setup

A. Experimental Device

The experimental device (Fig. 4) consists of four distinct parts: 1) the excitation source where the oxygen atoms are produced, 2) the test chamber where the oxygen atoms interact with the target, 3) the power controlling and monitoring devices needed to evaluate the heat balance, and 4) the atomic oxygen flux analysis by chemiluminescence.

Oxygen atoms are created in a low-pressure (300 Pa) plasma tubular reactor by a microwave 2450-MHz generator of 1000 W. The supplied gas is a high purity (99.998%) molecular oxygen, the flow rate is 1000 cm^3/min, and the dissociation rate is 4%.

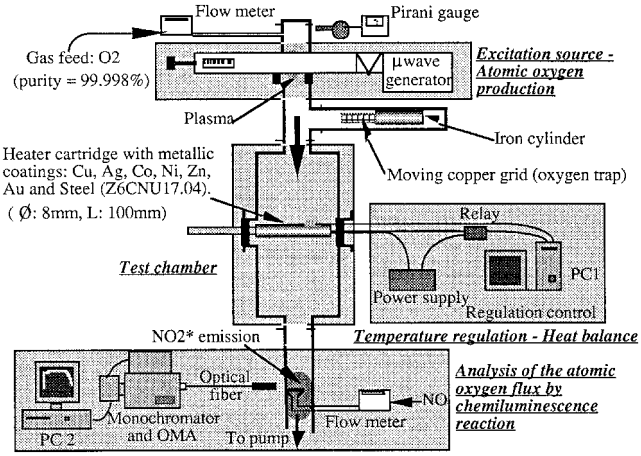

Fig. 4 Experimental setup for the accommodation coefficient determination by calorimetry measurements.

The plasma is created in a 25-mm-diam quartz tube. The test chamber in a Pyrex® glass cylinder (100 mm in diameter and 250 mm long) contains the target placed perpendicularly to the gas flux. Between the plasma source and the test chamber a copper grid that can recombine oxygen atoms allows the control of the atomic oxygen reaching the sample.

B. Metallic Samples Characterization

The test samples were stainless-steel heater cartridges with electrolytically deposited metallic coatings (buffer electrolysis).

Surface analysis of four coatings (Cu, Ag, Au, and Zn) were performed before oxygen plasma treatment to characterize the chemical surface state and to follow its evolution with the oxygen plasma exposition. The characterization of the coatings allows the evaluation of the oxidation degree of the metal before and after the treatment.

C. Temperature Regulation

A PID temperature regulation is used to maintain isothermal conditions in the heater cartridge. The power supply is stabilized and the energy is supplied to the heater by short pulses (50 ms) through an electronic switch (solid-state relay) controlled by a computer. In this way it was possible to regulate the temperature (by changing the number of pulses per second) and to measure the supplied power (by counting the number of pulses per second). The temperature is measured by a Pt 100 Resistance Temperature Detector probe placed at the opposite face of the cylinder with respect to the flow.

D. Analysis of the Atomic Oxygen Flux

The oxygen atoms flux is determined by a chemiluminescence method using nitric oxide (NO).[15–19] When nitric oxide molecules react with the oxygen atoms, the following reaction produces excited NO_2^* molecules:

$$NO + O + M \rightarrow NO_2^* + M$$

$$\text{with} \quad k_1 = 2.8 \times 10^{16}\ cm^6\ mol^{-2}\ s^{-1}$$

The NO_2^* de-excitations leads to a continuum emission between 380 and 1600 nm, with a maximum at 580 nm, or by collision with other species M:

$$NO_2^* \rightarrow NO_2 + h\nu \quad \text{(continuum)} \quad k_r = 10^5\ s^{-1}$$

$$NO_2^* + M \rightarrow NO_2 \quad k_q$$

In steady state, the intensity of the NO_2^* emission can be written as follows:

$$I_{NO_2^*} = k_r(NO_2^*) = \frac{k_r k_l (NO)(O)(M)}{k_r + k_q(M)} \quad (6)$$

Under a pressure greater than 0.1 torr, $k_r << k_q(M)$, Eq. (6) is simplified as follows[20]:

$$I_{NO_2^*} = k(NO)(O) \quad (7)$$

where $k = k_l k_r / k_q$. By plotting the emission intensity of NO_2^* at 580 nm vs the NO concentration, the slope of the straight line allows the determination of oxygen atoms concentration, knowing the constant k. However, this constant k depends only on the optical system and the wavelength; it is determined in a pure nitrogen discharge. For our experimental conditions, it gives $k = 1.95 \times 10^{-14}$ cm^3 s^2 mol^{-2}.

During the study, the atomic oxygen flux is titrated at the exit of the reactor by the injection of NO gas, whereas the NO_2^* continuum emission is collected via an optical fiber and analyzed by a monochromator and an optical multichannel analyzer (OMA). The signal can also be treated and viewed on a personal computer.

E. Experimental Procedure

The inlet gas is pure oxygen (99.998%) to measure only the recombination energy of atomic oxygen. The highest oxygen dissociation is obtained under the following experimental conditions: oxygen flow = 1000 cm^3/min, incident power of the microwave generator = 1000 W, pressure in the reactor = 300 Pa, and metal surface temperatures = 40 and 150°C.

For the oxygen atoms titration, the gas flow introduced is between 0 and 40 cm^3/min. The steady state for heat transfer is obtained after 90 min.

The heater cartridge is used as an isothermal calorimeter. In the first step of our measurement, the discharge is switched on, the oxygen atoms are recombined on a copper grid, and the system reaches its equilibrium temperature. The power needed for these isothermal conditions gives Q_1. Then, the copper grid is removed and the oxygen atoms reach the surface of the sample where they are partially recombined. The power needed for keeping the temperature constant in this case is Q_2 (Q_2 is lower than Q_1). The difference between the power required with and without oxygen atoms corresponds to the energy of atomic oxygen recombination released to the surface sample: $\delta Q = Q_1 - Q_2$. During the measurement, the radiation losses are always the same because the temperature remains constant. The temperature accuracy of 0.3°C allows a determination of the recombination energy with an error close to 1%. The accommodation coefficient is determined by the relation in Eq. (5). The concentration of oxygen atoms recombined on the surface is measured by NO titration at the reactor exit (Fig. 5). In a first time, the atomic oxygen flux without any sample is measured to determine the incident flux n_0. In a second time, the flux of oxygen atoms that have not recombined (n) is measured when the sample is kept at a constant temperature (40 or 150°C). The recombined oxygen atoms are then determined by the difference $n_0 - n = \Delta n$. The accuracy of Δn values established from the statistical error of the NO_2^* emission intensity is estimated at 9%.

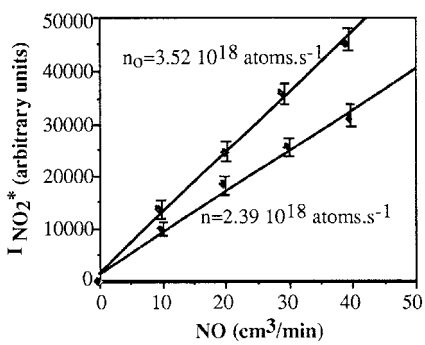

Fig. 5 NO_2^* emission intensity vs NO concentration for the oxygen atomic titration (n_o: number of oxygen atoms without any sample, n: number of oxygen atoms with a copper sample).

IV. Catalycity Results and Surface Aging

A. *b* Measurements on Metallic Coatings

For each metallic sample, the part of the recombination power transferred to the surface (δQ) and the flux of recombined oxygen atoms Δn have been measured at two different temperatures, 40 and 150°C (Table 1). The measured recombination powers transferred to the surface vary from 68×10^{-3} J s^{-1} for a nickel coating to 393×10^{-3} J s^{-1} for a silver coating, whereas the number of recombined atoms ranges from 3.90×10^{17} atoms s^{-1} for zinc to 1.13×10^{18} atoms s^{-1} for copper. Therefore, the mass and heat transfers depend on the nature of the materials.

Accommodation coefficients β were deduced from these measurements according to the relation in Eq. (5) (Table 2). For each sample, the measurements have been performed twice, allowing the verification of good reproducibility. The accuracy of the results is calculated from the experimental errors of the recombination power and the number of recombined oxygen atoms:

$$\frac{d\beta}{\beta} = \frac{d\delta Q}{\delta Q} + \frac{d\Delta n}{\Delta n} \quad (8)$$

As $d\delta Q/\delta Q = 0.09$ and $d\Delta n/\Delta n = 0.01$, the accuracy of the measurements is 10%.

The experimental values show that β depends on the nature of the material. For all metallic coatings, the accommodation coefficient increases with the surface temperature. That means that the O_2 molecules leave the surface by releasing a greater part of their recombination energy.

However, in the case of the silver coating, a decrease of β was observed for a surface temperature of 150°C. This result points out the chemical evolution of the surface during the

Table 1 Recombination powers and number of recombined oxygen atoms for each sample and surface temperature

	Surface temperature: 40°C		Surface temperature: 150°C	
Coatings	$\delta Q \pm 1\%$, 10^{-3} J s^{-1}	$\Delta n \pm 9\%$, 10^{17} atoms s^{-1}	$\delta Q \pm 1\%$, 10^{-3} J s^{-1}	$\Delta n \pm 9\%$, 10^{17} atoms s^{-1}
Copper	137	11.3	241	14.7
Silver	393	10.7	367	12.8
Cobalt	168	6.79	192	7.23
Gold	97	5.37	147	7.07
Zinc	86	3.90	157	6.73
Nickel	68	4.93	115	8.21
Steel	196	13.8	171	10.8

Table 2 b measurements of different metallic coatings for oxygen atoms at low pressure (300 Pa), evolution with the surface temperature

	β according to the surface temperature, °C	
Surface coating	40	150
Copper	0.30 ± 0.03	0.41 ± 0.03
Silver	0.91 ± 0.09	0.71 ± 0.08
Cobalt	0.61 ± 0.05	0.66 ± 0.06
Gold	0.45 ± 0.05	0.52 ± 0.05
Zinc	0.55 ± 0.03	0.58 ± 0.05
Nickel	0.34 ± 0.02	0.35 ± 0.03
Steel	0.36 ± 0.03	0.39 ± 0.03

Table 3 Accommodation coefficient measurements, comparison with literature results

	β, surface temperature 40°C		
Surface coating	This work	Melin and Madix[6]	Krech[12]
Copper	0.30 ± 0.03	0.30 ± 0.08	——
Silver	0.91 ± 0.09	0.95 ± 0.25	——
Cobalt	0.61 ± 0.05	0.67 ± 0.20	——
Gold	0.45 ± 0.05	0.17 ± 0.05	0.43 ± 0.12
Zinc	0.55 ± 0.03	——	——
Nickel	0.34 ± 0.02	0.16 ± 0.05	0.35 ± 0.12
Steel	0.35 ± 0.03	——	——

Table 4 Catalycity classification of several metals according to k_w

Surface coating	γ, ±20%	β, ±10%	β·γ, ±30%	k_w, cm s^{-1}, ±30%
Copper	2.5×10^{-2}	0.30	7.5×10^{-3}	121
Zinc	4.3×10^{-3}	0.55	2.4×10^{-3}	38
Gold	5.0×10^{-3}	0.45	2.2×10^{-3}	36
Silver	1.5×10^{-2}	0.91	1.4×10^{-2}	219
Steel	7.1×10^{-3}	0.36	2.6×10^{-3}	42

recombination phenomena. Indeed, an oxide layer (Ag_2O) was formed on the surface coating during the experiment. Under a 300 Pa pressure and a 150°C temperature, Ag_2O was vaporized in the gas bulk. Therefore, some recombination reactions of oxygen atoms occurred in the gas bulk. Because the reaction did not occur on the surface, the heat released to the material was lower. That can explain the decrease of the accommodation coefficient at this temperature.

Comparison of our results with the literature shows good agreement, except for Au and Ni where Melin and Madix[6] found β values to be three times lower (Table 3). The accuracy in our measurements has an error less than 10%, whereas Krech[12] and Melin and Madix[6] gave results with nearly a 30% error.

B. Catalycity Scale

The quantification of the mass and heat transfer resulting from the recombination of oxygen atoms can be evaluated by γ and β. The β·γ product of these two coefficients represents the total energy transferred to the surface and defines the catalycity of a material. Furthermore, a specific surface heating rate k_w, called *wall catalycity* by aerodynamicians, is defined as[21]

$$k_w = (kT/2\pi m)^{1/2}\beta\gamma \qquad (9)$$

For a surface temperature of 40°C, $(kT/2\pi m)^{1/2} = 160.83$ m s^{-1} and allows the establishment of a catalycity scale of the metals (Table 4). The resulting absolute catalycity scale obtained is

$$Ag > Cu > Steel > Zn > Au$$

This scale is in agreement with literature and allows us to validate the experimental setup and the measurement methods. It constitutes a reference for future studies on ceramic materials that have a large range of applications. According to the chemical state of the surface hypotheses, this catalycity scale is assumed to classify the pure metals. However, the following chemical analyses of the samples surface show their aging. And this aging occurs during the measurement.

C. Evidence of Surface Oxidation by ESCA Analyses

The plasma–surface interaction, and particularly the recombination reaction of the atomic oxygen, depends strongly on the chemical state of the surface material, and it is well known that the oxidation of the metal takes place in only a few milliseconds. That is why we have selected four coatings: two

Table 5 Inorganic oxygen content relating to the metal

	O_{linked} to the metal			
	Zinc	Gold	Silver	Copper
Nontreated, 200 ms	0.21	<0.01	0.16	——
Exposed, 12 s	0.17	<0.01	——	0.21
Exposed	0.18	<0.01	0.61	0.31

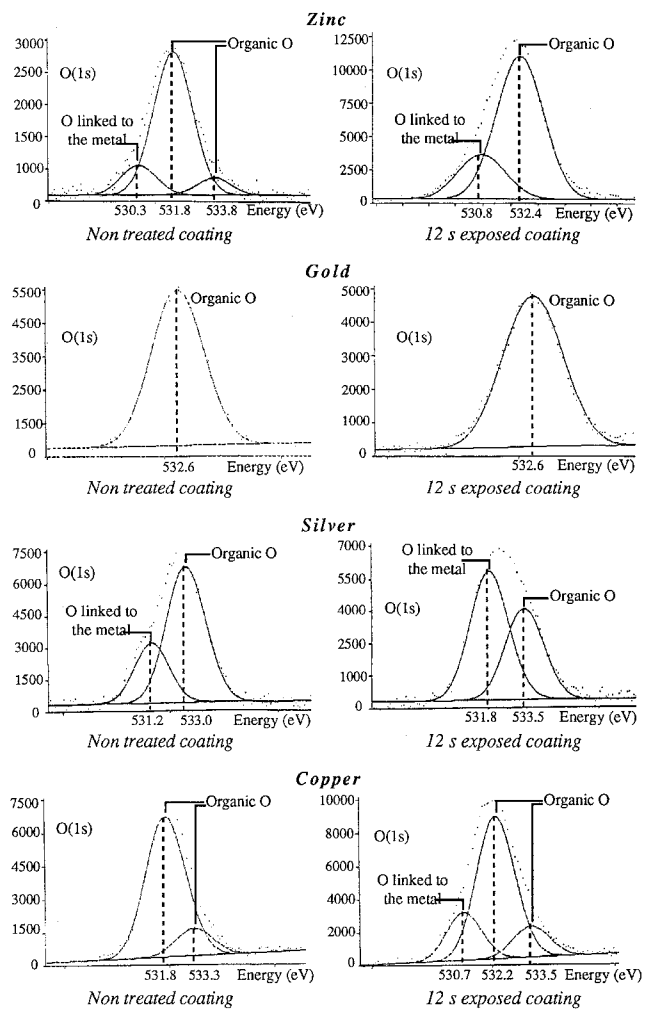

Fig. 6 O(1s) spectra of zinc, gold, silver and copper coatings; comparison between treated and nontreated samples.

strongly catalytic (copper and silver) and two poorly catalytic (gold and zinc), to follow their evolution with the plasma exposition time. ESCA was the analysis technique used.

This nondestructive analysis gives qualitative and quantitative information about surface species. The ESCA spectroscopy is based on the photoelectric effect. Samples are irradiated with x rays (1500 eV), and the kinetic energy of the ejected photoelectron enabled us to determine the bond energy between the electron and the atom, taking the surrounding electrons into account. The electronic energies were calculated with a precision of about 0.1 eV, and the thickness of the analyzed layer was about 5 nm.

For each electrolytically deposited metal, three groups of spectra were performed: 1) a nontreated sample, 2) a short-time-exposed (200-ms) sample, and 3) a long-time-exposed (12-s) sample. Each group of spectra includes the quantitative results (for oxygen, carbon, and metal), the global spectrum, the C(1s) and O(1s) peak, and the peak because of the metal. For each metal and treatment (short time, long time, or reference), the ratio $O_{\text{linked to the metal}}$/Metal was evaluated. This ratio can provide a correct quantitative approach (Table 5 and Fig. 6).

These analyses show that the catalycity of the materials depends on the degree of their oxidation. Indeed, gold, where no oxygen linked to the metal was found by ESCA, has a low catalycity. With zinc, the peak as a result of the oxygen linked to the metal remains stable during the treatment. Zinc is already oxidized before its exposition to the oxygen plasma as an ZnO oxide layer. In the case of catalytic samples, copper and silver, the inorganic oxygen proportion increases dramatically with the exposure time and the surfaces are oxidized as Cu_2O and Ag_2O, respectively.

In all cases, the chemical evolution of the metal surface cannot be neglected, essentially for the catalytic metals. Indeed, the formation of an oxide layer appears from the first exposure times, and then the oxidation mechanisms are stabilized. The catalycity of the metals also depends on their oxidation mechanism.

V. Discussion

The hypothesis of nonevolutive metallic surfaces was invalidated because the surface analyses ESCA showed an oxidation of the material from the first milliseconds of exposure to the atomic oxygen flux. Oxidation mechanisms and ablation of the material in the case of a silver surface must be taken into account. Also, the recombination reaction occurs on the oxide layer and, except for gold, which does not present any oxidation, the catalycity scale is established for the metallic oxides rather than for the pure metal. This ranking becomes as follows:

$$Ag_2O > Cu_2O > Fe_2O_3 > ZnO > Au$$

Another important point is to link the oxidation mechanisms and the catalytic behavior of the materials.

In usual temperature and pressure conditions, a thin oxide or sulphide layer of about 10 nm covers the surface of metals exposed to the air, except for some metals such as gold and platinum. According to Myerson,[22] the oxidation phenomena imply the chemisorption of molecular oxygen. However, the interaction of oxygen atoms with the surface leads to the formation of an oxide layer where the catalytic properties of the material appear. Moreover, because atomic oxygen has a greater chemical potential than molecular oxygen, the oxygen atoms take over the structures from molecular oxygen to form strongly linked species to the metal. Also, the oxide will control the recombination reaction by modification of the activation energy of the oxygen–metal bond.

The mobility of oxygen atoms during the oxidation process can influence the catalycity of the material. As a rule, the mobility of adsorbed oxygen atoms increases when the oxygen–metal bond energy becomes weaker. It also increases with the surface temperature. This mobility can be considered a result of a diffusion of the oxygen atoms or ions (O^- or O^+) on the metal surface.

The metallic oxides formed from the first exposure times to the oxygen flux have *n*- or *p*-type semiconductor properties. The catalytic reactivity of these oxides will depend on their electrical properties.

Catalycity results of atomic oxygen on a metallic surface are listed in Table 6. Relations between the catalycity of the materials and their electronic properties can be pointed out.

Indeed, the *n*-type electronic conductors as SiO_2, ZnO, WO_3, and Fe_2O_3 have a lower catalycity than *p*-type electronic conductors as Co_3O_4, Ag_2O, and Cu_2O. Moreover, the lower the width of the forbidden zone (E_{gap}), the higher the catalycity. Also, it seems that there is a relation between the electron's mobility in the material and its catalycity.

According to Weisz,[23,24] the coverage of adsorbed oxygen molecules is really higher for *p*-type oxides than for *n*-type oxides. We can suppose the same behavior for atomic oxygen. Indeed, the adsorption of an oxygen atom on an *n*-type semiconductor is because of the creation of surface ionic species using the lattice electrons. As the coverage of the surface increases, only few electrons can move to the surface because of the electrostatic repulsion between the surface and the moving electrons. The number of defects in this kind of oxide is a restricted factor. On the other hand, the oxygen adsorption on *p*-type oxides is a result of the creation of surface ionic species using the electrons released from charges separating, corresponding to moving holes. The surface coverage can also increase until saturation is complete.

The *p*-type conduction is the result of electron's transfer from the valence band to the conduction band allowing oxygen adsorption that creates electronic holes in the valence band.

Table 6 Catalycity of metallic surfaces and correlation with electronic properties of materials

	$k_w = \beta\gamma \left(\frac{kT}{2\pi m}\right)^{1/2}$, cm s^{-1}				
	This work, ±30%	Nguen-Xuan et al.,[5] ±30%	Melin and Madix,[6] ±60%	Semiconductor type	E_{gap}, eV
Co(Co_3O_4)	——	——	808	*p*	0, 9
Ag(Ag_2O)	219	193	3667	*p*	1.5
Cu(Cu_2O)	121	176	145	*p*	1.9
Zn(ZnO)	38	39	——	*n*	3.3
Ni(NiO)	——	——	44	*p*	1, 95
Au	36	——	22	——	——
Pt	——	——	23	——	——
Fe/Steel(Fe_2O_3)	42	——	11	*n*	1.9
W(WO_3)	——	——	19	*n*	2, 8
SiC(SiO_2)	——	6	——	*n*	11

The lattice oxygen atoms near the surface will also release some electrons, allowing oxygen adsorption and the creation of holes. At low temperature, the holes are trapped on the lattice ions and some O species are created. A holes concentration in the valence band can lead to the formation of covalent bindings as O–O. The electrons transfer from the valence band to the surface, to the conduction band, is easier if the width of the forbidden zone (E_{gap}) is small. Also, the surface coverage of oxygen increases and the catalycity of the material is higher.

The electronic and catalytic properties of NiO have been studied by Dickens and Sutcliffe.[25] It has been shown that recombination may possibly occur only on a few particularly active surface sites, and that on *p*-type semiconductors such sites may arise from the presence of underlying holes or from the delocalization of holes formed during adsorption. On the other hand, an underlying cation vacancy will inhibit the recombination of oxygen atoms on the surface.

In conclusion, the electronic properties of the metallic oxides formed during the oxygen plasma–metal interaction will influence the oxygen atoms adsorption on the surface. The catalycity of the oxide will depend sensitively on the *p* or *n* nature of the semiconductor. Thus, the *p*-type oxides, which have a high coverage of adsorbed oxygen atoms, will have a catalytic reactivity much more important than the *n*-type oxides.

Concerning silver, more complex mechanisms occur because of a strong oxidation of the surface and a no-neglected ablation of the material. Indeed, silver oxide Ag_2O formed during the interaction of the metallic surface with the atomic oxygen flux is a volatile compound at the working pressure (300 Pa), even for low temperatures (experiments at 40 and 150°C). The accommodation coefficient results have to be considered carefully because the measurements of the consumed oxygen atoms flux and the overheating of the surface are the results of recombination mechanisms and oxidation/ablation of the surface. Actually, the experimental devices and the measurements methods are unable to dissociate these phenomena. However, ablation of Ag_2O will lead to the formation of a gaseous Ag_2O (or AgO) layer near the surface. A fraction of oxygen atoms will recombine in the gas bulk before striking the surface. This process should lead to a decrease in the material overheating. The ablative layer would behave like a thermal protection of the underlying material. Indeed, the experimental measurements on the silver surface have shown a decrease of the accommodation coefficient when the temperature increases, that means when the ablation mechanisms are favored ($\beta = 0.91 \pm 0.03$ at 40°C, whereas $\beta = 0.71 \pm 0.03$ at 150°C).

VI. Conclusions

Hypotheses concerning the chemical structure of the materials have been expressed. Indeed, the assumption of a chemically nonevolutive surface after exposition to a dynamic atomic oxygen flux has been advanced. That means that the oxygen atoms that react on the surface will recombine to form molecular oxygen or return to the gas phase. However, surface analyses of the materials by ESCA showed the formation of a metallic oxide layer during the first hundred milliseconds of exposure to the plasma, and then the system was stabilized for longer times. As the time required for an experiment is long (about 60 min), the equilibrium of the oxidation mechanisms is supposed to be reached. The surface composition is also assumed to be stable during the measurement, even if the recombination reaction does not occur on the pure metal but on the metallic oxide layer instead.

The surface state having been defined, the accommodation coefficient measurements were performed on several metallic coatings such as copper, silver, zinc, gold, nickel, cobalt, and steel. The development of the experimental setup allowed improvement in the accuracy of the measurements at 10%, which is a main point to obtain significant results for each material. Thus, an absolute catalycity scale has been established to classify the materials according to their catalytic behavior in well-defined operating conditions. This classification constitutes a reference for future studies on other materials such as ceramic or a catalyst.

Finally, at the same time, an agreement with the literature on the electronic properties of the metallic oxides relationships between the catalycity of the material and its electronic nature has been established. Indeed, the *p*-type oxides like Ag_2O or Cu_2O are strongly catalytic, whereas the *n*-type oxides such as SiO_2 or ZnO are poorly catalytic. Moreover, the higher the optical gap the lower the catalycity of the semiconductor. Therefore, one can suggest that the displacement of the electrons in the material is highly correlated to the recombination processes, particularly during the adsorption phase of oxygen adsorbed by the creation of the O^- ionic species.

Acknowledgments

This work was financially supported by Centre National d'Etudes Spatiales, Evry, France and Dassault Aviation, St. Cloud, France.

References

[1]Warnatz, J., "Resolution of Gas Phase and Surface Combustion Chemistry into Elementary Reactions," *24th Symposium International on Combustion*, The Combustion Inst., Pittsburgh, PA, 1992, pp. 553–579.

[2]Deutschmann, O., Riedel, U., and Warnatz, J., "Modeling of Nitrogen and Oxygen Recombination on Partial Catalytic Surfaces," *Journal of Heat Transfer*, Vol. 117, No. 2, 1995, pp. 495–501.

[3]Willey, R. J., "Comparison of Kinetic Models for Recombination on High-Temperature Reusable Surface Insulation," *Journal of Thermophysics and Heat Transfer*, Vol. 7, No. 1, 1993, pp. 55–62.

[4]Seward, W. A., and Jumper, E. J., "Model for Oxygen Recombination on Silicon-Dioxide Surfaces," *Journal of Thermophysics and Heat Transfer*, Vol. 5, No. 3, 1991, pp. 284–291.

[5]Nguyen-Xuan, F., Mallard, O., Cavadias, S., Amouroux, J., Le Bozec, A., and Rapuc, M., "Catalycity Measurements on Metallic and SiC Material Surfaces in a Pulsed Plasma Reactor," *Proceedings of the 2nd European Symposium on Aerothermo-Dynamics for Space Vehicles*, edited by J. J. Hunt, European Space Agency, ESTEC-ESA, Noordwijk, The Netherlands, pp. 457–461.

[6]Melin, G. A., and Madix, R. J., "Energy Accommodation During Oxygen Atom Recombination on Metal Surfaces," *Transactions of the Faraday Society*, Vol. 67, part 1, 1971, pp. 198–211.

[7]Myerson, A. L., "Exposure-Dependent Time Surface Recombination Efficiencies of Atomic Oxygen," *Journal of Chemical Physics*, Vol. 50, No. 3, 1969, pp. 1228–1234.

[8]Nakada, K., "Recombination of Hydrogen, Nitrogen and Oxygen Atoms on Copper and Silver Single Crystal Surfaces," *Bulletin of the Chemical Society of Japan*, Vol. 32, 1959, pp. 1072–1078.

[9]Greaves, J. C., and Linnett, J. W., "The Recombination of Oxygen Atoms at Surfaces," *Transactions of the Faraday Society*, Vol. 54, Pt. 1, 1958, pp. 1323–1330.

[10]Scott, C. D., "Catalytic Recombination of Nitrogen and Oxygen on High-Temperature Reusable Surface Insulation," AIAA Paper 80-1477, July 1980.

[11]Zoby, E. V., Gupta, R. N., and Simmonds, A. L., "Temperature Dependent Reaction Rate Expressions for Oxygen Recombination at Shuttle Entry Conditions," AIAA Paper 84-0224, Jan. 1984.

[12]Krech, R. H., "High Velocity Atomic Oxygen/Surface Accommodation Studies," *Journal of Spacecraft and Rockets*, Vol. 30, No. 4, 1993, pp. 509–513.

[13]Kontinos, D., "Coupled Thermal Analysis Method with Application to Metallic Thermal Protection Panels," *Journal of Thermophysics and Heat Transfer*, Vol. 11, No. 2, 1997, pp. 173–181.

[14]Halpern, B., and Rosner, D. E., "Chemical Energy Accommodation at Catalyst Surfaces," *Journal of the Chemical Society Faraday Transactions I*, Vol. 74, No. 1, 1978, pp. 1883–1912.

[15]Stone, E. J., and Zipf, E. C., "Electron-Impact Excitation of $^3S^O$ and $^5S^O$ States of Atomic Oxygen," *Journal of Chemical Physics*, Vol. 60, No. 11, 1974, pp. 4237–4243.

[16]Smith, E. R., "Electron-Impact Excitation of Atomic Oxygen," *Physical Review A: General Physics*, Vol. 13, No. 1, 1976, pp. 65–73.

[17]Sawada, T., and Ganas, P. S., "Distorted Wave Calculation of

Electron-Impact Excitation of Atomic Oxygen," *Physical Review A: General Physics*, Vol. 7, No. 2, 1973, pp. 617–626.

[18]Julienne, P. S., and Davis, J., "Cascade and Radiation Trapping Effects on Atmospheric Atomic Oxygen Emission Excited by Electron Impact," *Journal of Geophysical Research*, Vol. 81, No. 4, 1976, pp. 1397–1403.

[19]Lawrence, G. M., "Dissociative Excitation of Some Oxygen-Containing Molecules: Lifetimes and Electron-Impact Cross Sections," *Physical Review A: General Physics*, Vol. 2, No. 2, 1970, pp. 397–407.

[20]Kaufman, F., "The Air Afterglow and Its Use in the Study of Some Reactions of Atomic Oxygen," *Proceedings of the Royal Society of London, Series A: Mathematical and Physical Science*, A247, 1958, pp. 123–139.

[21]Laidler, K. J., Glasstone, S., and Eyring, J., "Application of the Theory of Absolute Reaction Rates to Heterogeneous Processes," *Journal of Chemical Physics*, Vol. 8, 1940, pp. 659–676.

[22]Myerson, A. L., "Mechanisms of Surface Recombination from Step Function Flows of Atomic Oxygen over Noble Metals," *Journal of Chemical Physics*, Vol. 42, No. 9, 1965, pp. 3270–3276.

[23]Weisz, P. B., "Electronic Barrier Layer Phenomena in Chemisorption and Catalysis," *Journal of Chemical Physics*, Vol. 20, No. 9, 1952, pp. 1483, 1484.

[24]Weisz, P. B., "Effects of Electronic Charge Transfer Between Adsorbate and Solid on Chemisorption and Catalysis," *Journal of Chemical Physics*, Vol. 21, No. 9, 1953, pp. 1531–1538.

[25]Dickens, P. G., and Sutcliffe, M. B., "Recombination of Oxygen Atoms on Oxide Surfaces," *Transactions of the Faraday Society*, Vol. 60, No. 2, 1964, pp. 1272–1285.